Nanoscale

Combination targeting of 'platelets + fibrin' enhances clot anchorage efficiency of nanoparticles for vascular drug delivery

Journal:	*Nanoscale*
Manuscript ID	NR-ART-05-2020-003633.R1
Article Type:	Paper
Date Submitted by the Author:	10-Aug-2020
Complete List of Authors:	Sun, Michael; Case Western Reserve University, Biomedical Engineering Miyazawa, Kenji; Case Western Reserve University, Department of Biomedical Engineering Pendekanti, Tejal; Hathaway Brown School Razmi, Maya; Hathaway Brown School Firlar, Emre; University of Illinois at Chicago, Bioengineering Yang, Stephanie; Case Western Reserve University, Department of Biomedical Engineering Shokuhfar, Tolou; University of Illinois at Chicago, Department of Bioengineering; Michigan Technological University, Department of Mechanical Engineering Li, Oliver; Marshall University, Biomedical Sciences Li, Wei; Marshall University, Biomedical Sciences Sen Gupta, Anirban; Case Western Reserve University, Department of Biomedical Engineering

Combination targeting of 'platelets + fibrin' enhances clot anchorage efficiency of nanoparticles for vascular drug delivery

Michael Sun[1], Kenji Miyazawa[1], Tejal Pendekanti[2], Maya Razmi[2], Emre Firlar[3], Stephanie Yang[1], Tolou Shokuhfar[3], Oliver Li[4], Wei Li MD PhD[4], Anirban Sen Gupta PhD[1,*]

[1] Case Western Reserve University, Department of Biomedical Engineering, Cleveland, OH 44106, USA
[2] Hathaway Brown School, Shaker Heights, OH 44122, USA
[3] University of Illinois at Chicago, Department of Bioengineering, Chicago, IL 60607, USA
[4] Marshall University, Department of Biomedical Sciences, Huntington, WV 25755, USA

* Corresponding author:
Anirban Sen Gupta, PhD
Case Western Reserve University
Department of Biomedical Engineering
10900 Euclid Avenue, Cleveland, Ohio 44102
Email: axs262@case.edu

Abstract

Occlusive thrombosis is a central pathological event in heart attack, stroke, thromboembolism etc. Therefore, pharmacological thrombolysis or anticoagulation is used in treating these diseases. However, systemic administration of such drugs causes hemorrhagic side-effects. Therefore, there is significant clinical interest in strategies for enhanced drug delivery to clots while minimizing systemic effects. One such strategy is by using drug-carrying nanoparticles surface-decorated with clot-binding ligands. Efforts in this area have focused on binding to singular targets in clots, e.g. platelets, fibrin, collagen, vWF or endothelium. Targeting vWF, collagen or endothelium maybe sub-optimal since *in vivo* these entities will be rapidly covered by platelets and leukocytes, and thus inaccessible for sufficient nanoparticle binding. In contrast, activated platelets and fibrin are majorly accessible for particle-binding, but their relative distribution in clots is highly heterogenous. We hypothesized that combination-targeting of 'platelets + fibrin' will render higher clot-binding efficacy of nanoparticles, compared to targeting platelets or fibrin singularly. To test this, we utilized liposomes as model nanoparticles, decorated their surface with platelet-binding peptides (PBP) or fibrin-binding peptides (FBP) or combination (PBP + FBP) at controlled compositions, and evaluated their binding to human blood clots *in vitro* and mouse thrombosis model *in vivo*. In parallel, we developed a computational model of nanoparticle binding to single versus combination entities in clots. Our studies indicate that combination targeting of 'platelets + fibrin' enhances the clot-anchorage efficacy of nanoparticles while utilizing lower ligand densities, compared to targeting platelets or fibrin only. These findings provide important insights for vascular nanomedicine design.

1. Introduction

Vascular diseases leading to myocardial infarction (heart attack), stroke, pulmonary embolism etc. cause significant morbidities and mortalities in the US and globally.[1,2] Irrespective of the etiology of these diseases, a primary event in their pathophysiology is the formation of occlusive blood clots (thrombi) inside arteries and veins.[3-6] The development and growth of vascular thrombi involve three major aspects: (i) Adhesion of platelets at the vessel disease site (e.g. on inflamed endothelium, deposited von Willebrand Factor and exposed collagen), (ii) aggregation of activated platelets at the site predominantly by fibrinogen (Fg) binding to active platelet surface integrin αIIbβ3, and (iii) amplification of thrombin on the phosphatidylserine (PS) rich active platelet surface to convert blood protein fibrinogen (Fg) into fibrin which undergoes self-assembly and FXIIIa-mediated crosslinking to form an insoluble biopolymeric mesh securing the clot.[7-11] In physiological conditions, these clot formation mechanisms are essential in our body to promote hemostasis and prevent bleeding from vascular injuries. Post-hemostasis, during the healing phase, the fibrin clot is lysed by the action of plasmin which is generated from its zymogen plasminogen by the action of tissue plasminogen activator (tPA) secreted by the endothelium at the injury site.[12] Thus, in healthy physiological condition, clot formation and dissolution are highly regulated. However, in pathological conditions (e.g. atherosclerotic plaque rupture, coronary thrombosis, stroke, deep vein thrombosis, cancer etc.), the processes become dysregulated and occlusive blood clots lead to reduced blood flow, causing debilitating effects. In fact, in the recent global crisis stemming from COVID-19, coagulopathy and thrombosis have emerged as pertinent aspects of critically ill patients.[13,14]

Based on these pathologic mechanisms, pharmacological strategies have been developed to attenuate thrombus growth as well as to lyse dangerously occlusive thrombi. These strategies span across utilization of anti-platelet agents[15], anti-coagulant agents[16]and fibrinolytic agents.[17,18] Some of these strategies are currently being studied clinically for the treatment of COVID-19 patients.[19,20] Although these strategies are clinically well-established, all of these drugs are given systemically (e.g. oral or intravascular) and therefore result in various degrees of off-target side effects, especially internal hemorrhage.[21-27] As a result, there continues to be significant clinical interest in strategies that can enable enhanced drug delivery specifically targeted to the clot site while minimizing systemic side effects. We and others have recently comprehensively reviewed such approaches[28,29], where strategies for targeted drug delivery to clots have utilized either direct engineering of the drug to bear clot-anchoring motifs or packaging of the drug within nanoparticles that are surface-decorated with clot-anchoring motifs. In either case, the strategies have majorly focused on anchoring to a *singular* entity, e.g. to activated platelets or fibrin or vWF or exposed collagen or injured endothelium. We rationalize that drug or nanoparticle targeting to vWF or exposed collagen or endothelium may not be optimal for anchoring to clots, since in an occluded vessel the vWF, collagen and endothelium at the clot site may already be covered by platelets aggregated at the site and thus inaccessible for binding. In contrast, activated platelets and fibrin are spatiotemporally highly prevalent in clots, but their distribution is highly variable in arterial, venous and microvascular thrombi.[30-33] Therefore, singularly targeting ligand-modified drugs or ligand-decorated nanoparticles to platelets only or fibrin only may be sub-optimal to render sufficient clot-specific anchorage and accumulation. Figure 1 shows schematic illustration and experimental data of clot formation involving platelets and fibrin, with 1A showing schematic of vascular thrombosis, 1B comparing scanning electron microscopy (SEM) images and

immunofluorescence images of thrombus on non-clotting (albumin-coated) surfaces (B1, B3) vs. clot-promoting (collagen-coated) surfaces (B2, B4) exposed to human plasma *in vitro* in microfluidic chambers, and 1C comparing *ex vivo* SEM images of thrombus on uninjured (C1) vs. injured (C2) blood vessel wall in mice. These *in vitro* and *ex vivo* images clearly indicate that the 'platelets + fibrin' combination is always present at the site of thrombus development irrespective of heterogeneity in their distribution. Therefore, we hypothesized that combination targeting of 'platelets + fibrin' can render higher clot-binding efficacy of nanoparticles, compared to singularly targeting platelets only or fibrin only. To test this, we developed a computational model of nanoparticle binding to single versus combination entities in clots. In parallel, we utilized liposomes as model nanoparticles, decorated their surface with platelet binding peptides (PBP) or fibrin binding peptides (FBP) or combination (PBP + FBP) at controlled compositions, and evaluated their binding to human blood clots *in vitro* in a microfluidic system and *in vivo* in a mouse artery thrombosis model. The PBP sequence is derived from the active platelet αIIbβ3 binding GRGDS domain of fibrinogen and we have utilized this peptide previously to design liposomes that can specifically bind to activated platelets.[34] The FBP sequence was adapted from phage display libraries established for molecular imaging of fibrin, where it was demonstrated that this peptide motif has high selectivity and affinity for fibrin but not for fibrinogen.[35] We used such peptides for our targeting strategies instead of antibodies because: (i) peptides are less expensive than antibodies and can be custom-synthesized at large scale and high purity using solid phase peptide synthesizer[36]; (ii) small molecular weight peptides have much reduced secondary or higher conformations compared to proteins and antibodies and hence have reduced immunogenicity risks[37]; (iii) compared to small peptides large antibodies can sterically limit the number of copies that can be decorated on a nanoparticle surface.[38] Here we report our computational and experimental studies that indicate that combination targeting of 'platelets + fibrin' using corresponding peptide ligands can significantly enhance the clot-anchorage efficacy of nanoparticles while utilizing lower ligand densities compared to singularly targeting platelets only or fibrin only. Our findings provide important design insights for vascular nanomedicine systems.

2. Materials and Methods

2.1. Materials

For liposomal nanoparticle fabrication, distearoyl phosphotidyl choline (DSPC), methoxy polyethylene glycol-conjugated distearoyl phosphotidyl ethanolamine (DSPE-mPEG$_{2000}$) and maleimide-terminated polyethylene glycol-conjugated distearoyl phosphotidyl ethanolamine (DSPE-PEG$_{2000}$-Mal) were purchased from Avanti Lipids (Alabaster, USA). N-succinimide-terminated polyethylene glycol-conjugated distearoyl phosphotidyl ethanolamine (DSPE-PEG$_{2000}$-NHS) was purchased from Nanosoft Polymers (Winston-Salem, USA). For microfluidic studies, the parallel plate flow chamber (PPFC) was purchased from Glycotech (Gaitersberg, USA). Polycarbonate membrane filters with 200 nm pore distribution, calcium chloride, and cholesterol were purchased from Sigma Aldrich (St. Louis, USA). Rhodamine-B-dihexadecanoyl-sn-glycero-3-phosphoethanolamine (DHPE-RhB, red fluorescence, λ_{ex} = 561, λ_{em} = 582) was purchased from Setareh Biotech (Eugene, USA). Thrombin was purchased from Haematologic Technologies (Essex Junction, USA). Phosphate buffered saline (PBS), collagen type I from rat tail, Calcein-AM (green fluorescence, λ_{ex} = 488, λ_{em} = 520) and AlexaFluor 647-conjugated

fibrinogen (deep red fluorescence, λ_{ex} = 650, λ_{em} = 665) were purchased from Thermo Fisher Scientific (Waltam, USA). For platelet binding peptide (PBP) the sequence *CGSSSGRGDSPA* that binds to activated platelet surface integrin αIIbβ3[34] was used, and for fibrin binding peptide (FBP), the sequence *cyclo-AC-Y(DGI)C(HPr)YGLCYIQGK-Am*[35] was used. Both peptides were custom synthesized by Genscript (Piscataway, USA). For in vivo studies on mice, anesthesia agents ketamine was obtained from Fort Dodge Animal Health, IA, USA and xylazine was obtained from Hospira, IL, USA. Ferric chloride ($FeCl_3$) for the carotid artery thrombus induction was purchased from Sigma. Intravital microscopy was carried out using a Leica DMLFS fluorescent microscope with a Gibraltar Platform (EXFO, Quebec, Canada). For *ex vivo* studies with human blood samples, human blood was obtained from healthy consenting donors using venipuncture protocol approved by the Case Western Institutional Review Board (IRB), titled 'Analysis of Nanoparticle Interactions with Blood Cells' (STUDY 20191092). For *in vivo* studies to test nanoparticle binding to arterial thrombosis in a mouse model, all procedures were carried out using protocol approved by the Institutional Animal Care and Use Committee (IACUC) at Marshall University entitled "Mechanistic Role of Thymidine Phosphorylase in the Development of Chronic Diseases (IACUC #1033528)" that includes the $FeCl_3$-induced carotid artery thrombosis model in mice. Therefore all *ex vivo* experiments with human blood samples and *in vivo* experiments in mouse models were carried out in accordance with IRB and IACUC ethical guidelines approved at Case Western Reserve University and Marshall University respectively. Informed consent was obtained from all healthy human subjects regarding blood donation.

2.2. Computational model for binding of nanoparticles to platelets and fibrin in thrombus

Using MATLAB, a computational model was constructed to theoretically assess the potential benefit of combination binding to 'platelets + fibrin' versus binding to platelets only or fibrin only, in the context of nanoparticle binding to thrombus. For this analysis, the following simple assumptions were made: (i) the system is closed and well-mixed and the binding is at equilibrium, (ii) there are no environmental influence (e.g. temperature, pressure) on the system, (iii) the nanoparticles within the system were flowed over a 2D clot surface in a closed loop. The binding of the particles to the receptors was modeled as steady-state particle-receptor kinetics to form particle-receptor complexes. Six 'species' were considered in the analysis: platelets, fibrin, particles, 'particle + platelet' complexes, 'particle + fibrin' complexes, and 'particle + platelet + fibrin' complexes. In the system, it was assumed that the interaction of particles to receptors only occurred in a limited region near the clot, termed as the *reaction zone*[36], and that there were no nanoparticles within the reaction zone initially at time = 0. Within the reaction zone, nanoparticles can associate to the clot or dissociate back into the bulk flow of nanoparticles within the system. The kinetic rate for nanoparticle flow was determined by the flow chamber dimensions (4 cm x 1 cm x 0.025 cm), shear stress (25 dyn/cm^2), flow rate (22.1 mL/min), and theoretical diffusivity of nanoparticles of 100nm-200 nm diameter dimension (1 x 10^{-5} cm^2/s).[39,40] It was assumed that the initial and subsequent binding of the ligands on particles to their corresponding receptors operated on first-order kinetics, and would not affect the subsequent binding of other ligands to their receptors (each individual binding reaction was independent from each other). The reverse and forward reaction rates for each ligand as well as initial concentration for the platelet and the fibrin was adapted from literature[35,41], and the concentration of particle-receptor complexes were plotted over 30 minutes. For the model, the concentration of particle-receptor complexes was defined as

a ligand-receptor interaction where ligands on particles could bind to different species dependent on the condition modeled. The association and dissociation rate constants used in the model were also adapted from literature. For PBP binding to platelet αIIbβ3, k_{on} was 3 x 10^9 $M^{-1}\cdot s^{-1}$ and k_{off} was 1.43 s^{-1}, and for FBP binding to fibrin, k_{on} was 3.33 x 10^5 $M^{-1}\cdot s^{-1}$ and k_{off} was 1 s^{-1}.[35,39,41] Platelet αIIbβ3 and fibrin concentrations (2.7 x 10^{15} receptors per mL and 4.4 x 10^{15} receptors per mL, respectively) were calculated from average platelet number in platelet-rich plasma (3.5 x 10^9 platelets per mL)[42], average αIIbβ3 receptors per platelet (80,000 receptors per platelet)[43], and average fibrinogen concentration in blood plasma (2.5 mg/mL)[44], respectively. The total number of particles within the system (3 x 10^{11} particles per mL) and receptors were maintained at a constant concentration throughout each condition. For the combination targeting particles, the particle species had both fibrin-targeting and platelet-targeting ligands at half of the concentration that the singularly targeting particles (platelet targeting only or fibrin targeting only) had, while maintaining the total number of particles constant. We also computed the binding profile for the condition where two different singularly targeting particles (platelet targeting and fibrin targeting) were mixed together (i.e. PBP-decorated particle and FBP-decorated particles are mixed together at 1:1 ratio) with equal amounts of each particle. The equations used are as follows:

$$\frac{d[N]}{dt} = -k_{on,P}[N][P] + k_{off,P}[NP] - k_{on,F}[N][F] + k_{off,F}[NF] + k_{flow}[N_{out}] - k_{flow}[N]$$

$$\frac{d[P]}{dt} = -k_{on,P}[N][P] + k_{off,P}[NP] - k_{on,P}[NP][P] + k_{off,P}[NP_2] - k_{on,P}[NF][P] + k_{off,P}[C]$$

$$\frac{d[F]}{dt} = -k_{on,F}[N][F] + k_{off,F}[NF] - k_{on,F}[NF][F] + k_{off,F}[NF_2] - k_{on,F}[NP][F] + k_{off,F}[C]$$

$$\frac{d[NP]}{dt} = k_{on,P}[N][P] - k_{off,P}[NP] - k_{on,P}[NP][P] + k_{off,P}[NP_2] - k_{on,F}[NP][F] + k_{off,F}[C]$$

$$\frac{d[NF]}{dt} = k_{on,F}[N][F] - k_{off,F}[NF] - k_{on,F}[NF][F] + k_{off,F}[NF_2] - k_{on,P}[NF][P] + k_{off,P}[C]$$

$$\frac{d[NP_2]}{dt} = k_{on,P}[NP][P] - k_{off,P}[NP_2]$$

$$\frac{d[NF_2]}{dt} = k_{on,F}[NF][F] - k_{off,F}[NF_2]$$

$$\frac{d[C]}{dt} = k_{on,F}[NP][F] - k_{off,F}[C] + k_{on,P}[NF][P] - k_{off,P}[C]$$

$$\frac{d[N_{out}]}{dt} = -k_{flow}[N_{out}] + k_{flow}[N]$$

where N are nanoparticles in close proximity to the clot within the 'reaction volume', N_{out} are the remaining nanoparticles within the system distal to the clot, P are *available* platelet αIIbβ3 receptors for nanoparticle to bind, F are *available* fibrin receptors for nanoparticles to bind, NP are platelet-nanoparticle complexes, NP_2 are platelet-nanoparticle-platelet complexes, NF are fibrin-nanoparticle complexes, NF_2 are fibrin-nanoparticle-fibrin complexes, C are fibrin-nanoparticle-platelet complexes, $k_{on,P}$ and $k_{off,P}$ are the forward and reverse reaction rate constants for PBP to platelet αIIbβ3 receptors respectively, $k_{on,F}$ and $k_{off,F}$ are the forward and reverse reaction rate constants for FBP to fibrin respectively, and k_{flow} describes the transport of nanoparticles into the reaction zone.

2.3. Preparation and characterization of ligand-decorated liposomal nanoparticles

Figure 2A shows the schematic of heteromultivalently decorated nanoparticles that can enable combination targeting of 'platelets + fibrin' via specific binding to activated platelet integrin αIIbβ3 and to fibrin. For specific binding to platelet αIIbβ3, the PBP sequence *CGSSSGRGDSPA* was conjugated to DSPE-PEG_{2000}-Mal through thioether chemistry via the cysteine on the N-terminus of the peptide. The FBP sequence *cyclo-AC-Y(DGI)C(HPr)YGLCYIQGK-Am* was conjugated to DSPE-PEG_{2000}-NHS through amide chemistry via the N-terminus of the peptide. The DSPE-PEG_{2000}-PBP and DSPE-PEG_{2000}-FBP conjugations were confirmed by mass spectrometry. DHPE-RhB, cholesterol, and DSPE-PEG-peptide conjugates were dissolved in 1:1 chloroform : methanol, and liposomal nanoparticles were formed using film rehydration extrusion technique[45] utilizing a pneumatically controlled extruder and 200 nm pore size polycarbonate membranes (schematic in Figure 3A). The liposome size extrusion range was selected based on reported size of clinically approved liposomal formulations (e.g. Doxil and Ambisome liposomes are ~ 100 nm diameter, Myocet liposome is 150-250 nm in diameter, and Visudyne liposome is 150-300 nm in diameter). The liposomes were extruded 5 times per batch preparation. For various liposomal nanoparticle formulations, cholesterol and DHPE-RhB content were kept constant at 45 mol% and 1 mol % of total lipid respectively. The cholesterol mol% was chosen based on literature that cholesterol content of 30-50 mol% provides the highest membrane stability in liposomal vesicles.[46] For studies involving 'singular targeting' (platelets only or fibrin only) at various PBP or FBP densities on the nanoparticles, DSPE-PEG_{2000}-PBP or DSPE-PEG_{2000}-FBP content was varied at 2.5, 5, 7.5, or 10 mol % of total lipid. For studies involving 'combination targeting' ('platelets + fibrin'), DSPE-PEG_{2000}-PBP and DSPE-PEG_{2000}-FBP conjugates were combined at 1:1 ratio while keeping the total DSPE-PEG_{2000}-peptide content at 2.5, 5, 7.5, or 10 mol % of total lipid. Additionally, for effect of relative ligand ratio in combination targeting, DSPE-PEG_{2000}-PBP to DSPE-PEG_{2000}-FBP ratio was varied at 80:20, 60:40, 50:50, 40:60, 20:80, while keeping the total DSPE-PEG_{2000}-peptide content at 5 mol % of total lipid. The remainder of the mole% for all such formulations was DSPC lipid. Post-extrusion, the liposomal nanoparticles were characterized by dynamic light scattering (DLS) and cryo-transmission electron microscopy (cryo-TEM) for their size distribution, and zeta potential was characterized by a Malvern Zetasizer instrument.

2.4. Evaluation of nanoparticle binding to human blood clots in vitro

All studies with human blood and plasma samples were carried out with human blood drawn from healthy volunteer donors in accordance with protocols approved by CWRU Institutional Review Board. Human whole blood was centrifuged at 150g at 25°C for 10 min to obtain platelet-rich plasma (PRP). The platelets in the PRP were stained with calcein AM stained and the PRP was supplemented with 5% v/v AlexaFluor-647 fibrinogen. For each clot binding study, 50 µL of PRP was placed on a collagen-coated glass slide along with 250 nM thrombin in 0.5 M $CaCl_2$ to induce clot formation via concurrent platelet activation and fibrinogen-to-fibrin conversion. The glass slides with such clots were vacuum sealed inside the PPFC microfluidic chamber and liposomal nanoparticles (3×10^{11} nanoparticles/mL) were flowed over it approximately 20 ml/min (shear rate $\sim 2800\ s^{-1}$) leading to a theoretical shear stress of 25 dyn/cm^2 (theoretical calculation based on assuming plasma viscosity to be ~1cP at room temperature). The flow was maintained in a recirculating closed loop over the clot for 30 minutes, following which the clot was exposed to flow of PBS in an open loop for additional 5 minutes to wash off loosely-bound and unbound particles. Images of the clot were collected at various time points (0, 15 or 30 min of flow) using an inverted fluorescent microscope to capture particle fluorescence (RhB), platelet fluorescence

(Calcein AM) and fibrin fluorescence (AlexaFluor 647). For image analysis, surface-averaged fluorescence intensity of the nanoparticles (RhB) was quantified and normalized to the surface-averaged fluorescence intensity of fibrin (AlexaFluor 647) (n = 30 per condition). At the end of the experimental period, the slides bearing the 'nanoparticle (RhB) + platelets (Calcein) + fibrin (AlexaFluor-647)' in the clots were additionally analyzed under a confocal fluorescence microscope (Olympus FV1000) to obtain high resolution images of the clot-bound nanoparticles.

2.5. Nanoparticle binding to mouse carotid artery thrombus model in vivo

The mouse model experiments were carried out in accordance to Marshall University IACUC-approved protocols, using a ferric chloride ($FeCl_3$)-induced vascular injury and thrombosis model. This model of acute arterial thrombosis is well established in the literature[47], and we have previously utilized this model successfully to evaluate platelet-targeted nanomedicine.[48,53] For this, 8-12 weeks old week old C57BL/6 mice were first anesthetized with ketamine (100 mg/kg)/xylazine (10mg/kg), depth of anesthesia confirmed by toe-pinching, before surgically exposing the right carotid artery. A piece of filter paper soaked in 7.5% $FeCl_3$ solution was placed directly onto the carotid artery for 1 min. The $FeCl_3$ induces oxidative damage to the vessel wall, leading to endothelial injury and rapid thrombus formation within minutes (schematic illustration shown in Figure 9A). RhB-labeled platelet-targeted or fibrin-targeted or 'platelet + fibrin'-targeted liposomal nanoparticles at 150 µl injection volume were injected through the left jugular vein of the mouse (n = 3 per ligand decoration), and nanoparticle binding to the clot was observed and imaged in real time using a Leica DMLFS intravital fluorescent microscope with a Gibraltar Platform (EXFO, Quebec, Canada).

2.6. Statistical analysis

For in vitro clot-binding studies of nanoparticles, Brown-Forsythe and Welch ANOVA tests were used for the statistical analysis (based on quantification of nanoparticle RhB intensity normalized to fibrin AlexaFluor 647 intensity), and significance was considered for $p < 0.05$. Comparisons were carried out between singularly targeted (platelet-targeting only or fibrin-targeting only) nanoparticles at increasing ligand densities, versus combination targeted nanoparticles versus mixed singularly targeting nanoparticles. Comparison was also done for combination targeted nanoparticles with varying relative ratios of PBP:FBP content at 5 mol% total peptide content.

3. Results

3.1. Computational model of singular vs combination targeting of nanoparticles

For singular targeting to platelets only or fibrin only, we deem our nanoparticle design 'homomultivalent' (i.e. multiple ligands binding to a singular target entity) and for combination targeting we deem our nanoparticle design 'heteromultivalent' (i.e. multiple ligands binding to different target entities). In the model (see Methods for model description), concentration of homomultivalent particles (targeting platelets only or fibrin only) vs heteromultivalent particles (targeting platelets plus fibrin) vs mixture of homomultivalent particles (platelet-targeting only mixed with fibrin-targeting only) were computed over time as they approached equilibrium binding to clots rich in 'platelets + fibrin' (Figure 4). The computational output showed that over

a 30 min time period fibrin-targeting homomultivalent system led to slightly higher concentration of particle-receptor complexes compared to platelet-targeting homomultivalent system, while the 1:1 mixture of these two homomultivalent systems led to a higher extent of ligand-receptor complexes compared to either of the singularly targeted homomultivalent systems. During that same time period, the combination targeting (heteromultivalent) system reached the highest concentration of ligand-receptor complexes compared to either of the singular targeting (homomultivalent) systems or mixture of the homomultivalent systems. The heteromultivalent combination targeting condition also led to a slightly faster rate of binding (steeper slope) compared to the individual homomultivalent or mixed homomultivalent systems. Interestingly, the fibrin-targeting homomultivalent system showed a slightly slower rate of binding compared to all other targeting systems, at early time points (see inset of Figure 4 for 1 min time-period data). These data imply that the initial rate of binding of nanoparticles is faster for PBP-mediated binding to platelet αIIbβ3 (for singularly platelet-targeting, mixed homomultivalent targeting as well as heteromultivalent combination targeting) compared to FBP mediated binding to fibrin. This is because, in our current model, the PBP has a lower k_d (higher affinity) compared to the FBP, which when presented in multiple copies on the nanoparticle surface also results in overall higher avidity as has been demonstrated in multivalently decorated nanoparticles.[44] Thus, the binding rates at the initial stages would be dependent on individual ligand-receptor affinity parameters as well as the overall 'ligand density' on particles, while over time the extent of nanoparticle binding is favored more towards the higher probability of simultaneous anchorage to multiple target entities. Therefore, over time the 'mixed targeting' and the 'combination targeting' systems achieve higher levels of target-bound nanoparticles compared to singular targeting systems and combination targeting of nanoparticles to 'platelets + fibrin' appears to be the most efficacious.

3.2. Characterization of clot-targeted liposomal nanoparticles

Figure 2B shows MALDI-TOF mass spectroscopy results for PBP, FBP, DSPE-PEG_{2000}-Maleimide, DSPE-PEG_{2000}-Succinimidyl ester, and the resultant DSPE-PEG_{2000}-PBP and DSPE-PEG_{2000}-FBP conjugates that lead to corresponding designs of platelet-targeted, fibrin-targeted or combination-targeted liposomal nanoparticle systems. As evident from the results, the peptide conjugations were successfully achieved and a small fraction of free peptide or di-peptide remained in the reaction product. This free peptide or di-peptide fraction is ultimately eliminated when the DSPE-PEG_{2000}-peptide conjugates are finally utilized to make liposomal nanoparticles via film hydration and extrusion technique (Figure 3A) and the nanoparticles are isolated via column separation. Figure 3B shows representative morphology and size-characterization results of liposomal nanoparticles thus prepared, with B1 and B3 showing cryo-TEM and DLS data for multilamellar vesicles pre-extrusion, and B2 and B4 showing that for unilamellar vesicles post-extrusion. As evident from the data, the final nanoparticles had a diameter of approximately 168 nm. Zeta potential of the liposomal nanoparticles was determined to be -23.24 ± 6.8 mV. The PBP-decorated, FBP-decorated or 'PBP + FBP'-decorated liposomal nanoparticles this prepared, were used to carry out the clot-targeting experiments in the microfluidic set-up.

3.3. Effect of ligand density on singularly targeted vs. combination targeted nanoparticle binding to clots

Figure 5 shows representative confocal fluorescence images and surface-averaged RhB fluorescence intensity (hence extent of nanoparticle binding) data for liposomal nanoparticles bearing increasing mole % of PBP vs FBP vs '1:1 PBP : FBP'. Figure 5A shows this for PBP-decorated nanoparticles (i.e. platelet-targeting only) bound to clots at 30 min after flow is initiated, with PBP content at 2.5 mole % (A1), 5 mole % (A2), 7.5 mole % (A3) and 10 mole % (A4), as well as corresponding RhB fluorescence intensity (hence clot-bound nanoparticle) data at 15 min (A5) and 30 min (A6) after flow is initiated in the microfluidic chamber. As evident from the images and quantitative data, the binding of PBP-decorated (platelet-targeted) nanoparticles seem to increase with increasing extent of peptide content. In contrast, corresponding images and data shown in Figure 5B, B1-B6, for FBP-decorated (fibrin-targeted) nanoparticles suggest that the clot-binding efficacy of FBP-decorated nanoparticles increases when FBP content is increased from 2.5 mole % to 5 mole %, but beyond that the binding is not further increased with increasing FBP content and reaches a plateau. Most interestingly, as shown in Figure 5C, C1-C6, when 'PBP + FBP'- decoration (combination targeting) is used at 1:1 PBP:FBP ratio, the nanoparticle binding to clots significantly increases in going from 2.5 mole % total peptide to 5 mole % total peptide, but then decreases with increasing mole % of total peptide. Additionally, as shown in Figure 6, for 2.5 mole % (Figure 6. A1, A2) and 5 mole % (Figure 6. B1, B2) total peptide content, combination targeted ('PBP + FBP'- decorated) nanoparticles showed significantly higher clot-bound RhB fluorescence (hence higher clot-anchorage capability) compared to PBP-decorated or FBP-decorated nanoparticles. In fact, the extent of RhB fluorescence (hence clot-anchorage capability) for nanoparticles bearing 5 mole % 'PBP + FBP' at 1:1 ratio was significantly higher than that for nanoparticles bearing 7.5 mole % or 10 mole % PBP only or FBP only (shown for 15 min post-flow time point in Figure 6. C1 and 30-min post-flow time point in Figure 6. C2). Altogether, these findings suggest that combination targeting of 'platelets + fibrin' can achieve substantially higher clot-anchorage efficacy of nanoparticles compared to singularly targeting platelets only or fibrin only, while utilizing lower overall peptide content.

3.4. Comparing clot-binding efficacy of combination targeted nanoparticles to mixture of singularly targeted nanoparticles at equivalent ligand content

Since the combination targeted ('PBP + FBP'-decorated) nanoparticles bearing 5 mole % total peptide content (at 1:1 PBP : FBP ratio, 2.5 mole % of each) showed substantially higher clot-binding ability than singularly targeted nanoparticles bearing 5 mole % PBP or 5 mole % FBP only, we studied whether physically mixing the two singularly targeted nanoparticles at 1: 1 ratio would perform similarly to the combination targeted nanoparticles while keeping the total particle number fixed at 3×10^{11} nanoparticles per mL. As shown in Figure 7, representative fluorescence images (A1-A5) as well as quantitative analysis of clot-associated RhB fluorescence (hence clot-anchorage of nanoparticles) at 15 min (Figure 7B1) as well as 30 min (Figure 7B2) of flow, physically mixing singularly targeted (i.e. platelet-targeted only and fibrin-targeted only) nanoparticles at 1:1 ratio resulted in significantly higher overall clot-anchorage of nanoparticles compared to platelet-targeted only or fibrin-targeted only conditions. However, the nanoparticles simultaneously bearing both platelet-targeting and fibrin-targeting motifs (combination targeted) resulted in a significantly higher clot-anchorage capability than the physically mixed singularly targeted conditions. These results suggest that at 5 mole % total peptide content and fixed particle concentration 3×10^{11} nanoparticles per mL, combination targeting of 'platelets + fibrin' using heteromultivalent decoration of 'PBP + FBP' on a single nanoparticle system can achieve higher

clot-binding efficacy than physically mixing 'platelet targeting' and 'fibrin targeting' nanoparticles together at 1: 1 ratio.

3.5. Effect of relative ligand ratio on clot binding in combination targeted nanoparticles

Since the previous studies indicated that combination ('platelets + fibrin') targeting nanoparticles at 5 mole % total peptide ligand content (i.e. bearing 1:1 ratio of PBP : FBP at 2.5 mole % each) have the highest binding ability to clots compared to singularly (platelets only or fibrin only) targeted nanoparticles (i.e. bearing 5 mole % PBP only or FBP only), as well as compared to mixture of such singularly targeted nanoparticles, we further studied how varying the relative ratio (PBP : FBP) of ligands at 5 mol% total ligand content impacts the high clot-binding efficacy of combination targeted nanoparticles. Figure 8A shows representative confocal fluorescent images of RhB-labeled nanoparticles bearing 5 mol% ligands at PBP: FBP ratios of 5:0, 4:1, 3:2, 2.5:2.5, 2:3, 1:4 and 0:5, bound to clots at the 30 min time point in the microfluidic set-up at 25 dyn/ cm^2 shear stress flow conditions. Figure 8B shows quantitative analysis of the RhB fluorescence intensity (hence clot-binding extent of nanoparticles) with these various ligand ratios at the 15-min and 30-min time points. As evident from the images and quantitative results, the clot-binding ability of combination targeted nanoparticles bearing total 5 mole % ligand is maximized when PBP: FBP ratio reaches approximately 1:1 (shown here as 2.5: 2.5 mole %). This suggests that for combination targeting nanoparticles, co-decorating nanoparticles with equivalent densities of platelet-binding and fibrin-binding motifs provides the highest advantage and binding efficacy tapers off as the ligand combinations are biased more towards platelet- or fibrin-targeting only.

3.6. In vivo nanoparticle binding ability to arterial thrombus in mouse

Since our in vitro microfluidic studies indicate that nanoparticles bearing 'PBP + FBP' ligands for combination targeting of 'platelets + fibrin' undergo significantly higher clot-binding efficacy than nanoparticles bearing PBP only or FBP only for singularly targeting platelets or fibrin respectively, we evaluated the feasibility of this higher clot-binding efficacy in vivo in a $FeCl_3$-induced carotid artery thrombosis model in mice. Here, nanoparticle anchorage to the thrombus was observed in real time under intravital fluorescence microscopy. Figure 9B shows representative images and quantitative intensity data for thrombus-anchored nanoparticle RhB fluorescence over a 10 min period post $FeCl_3$-induced injury to blood vessel wall. It is important to note here that the fluorescence observed is entirely from nanoparticles bound to clots, as no other clot-associated entities (platelets, fibrin) were fluorescently labeled in these studies. As evident from the results, combination targeted nanoparticles showed higher fluorescence intensity compared to the singularly targeted nanoparticle conditions. It is important to note here that in these in vivo studies the observation time period was terminated at 10 min since these animals were not being treated with any thrombolytic drug and by 10 min time-point the blood vessel was majorly thrombo-occluded. These results indicate that the advantage of combination targeting of clots demonstrated in the microfluidic studies in vitro, remains valid in vivo.

4. Discussion

Nanoparticle-based therapeutic targeting of diseases to enhance site-specific drug availability and efficacy while avoiding non-specific drug distribution and side effects has emerged as a promising area of pharmaceutical development.[49,50] In majority of cases, these approaches focus on designing nanoparticles capable of binding to singular entities that are uniquely upregulated or exposed at the disease site. This design approach is labeled as 'homomultivalent targeting' since in this approach the nanoparticles are decorated with multiple copies of ligands directed to a single type of target entity. While this approach has shown promising results in disease site-specific binding of nanoparticles, the efficacy of nanoparticle binding can be affected by the high variability of expression or presence of the singular target entity. Realistically, in many disease scenarios, multiple types of target entities may be expressed or exposed simultaneously but at variable distribution patterns at the disease site. In such framework, simultaneously binding to multiple types of target entities via multiple copies of corresponding ligands can enhance the probability (hence extent) of nanoparticle binding to the disease site. This design approach is labeled as 'heteromultivalent targeting' and we have previously reviewed and demonstrated the advantages of this approach in several different disease scenarios.[51] A recent computational study has further emphasized the advantage of viewing the disease specific heterotypic 'target entity' profile as a 'bar code' that can be selectively recognized by corresponding heteromultivalent ligand decoration profile on the 'drug delivery' nanoparticle.[52]

Based upon the above rationale, here we studied whether combination targeting 'platelets + fibrin' provide enhanced clot-binding efficacy of nanoparticles, compared to singularly targeting platelets only or fibrin only. The motivation behind choosing platelets and fibrin as target entities stems from that fact that platelets and fibrin are the most prevalent components of a thrombus, even though their relative distribution may vary widely between arterial vs venous vs microvascular clots. Microparticle or nanoparticle targeting to platelets (via particle binding to single type of receptors or multiple types of receptors on platelet surface) has been extensively studied by our group and others, while nanoparticle targeting of fibrin has been studied by several research groups to achieve delivery of drugs or imaging agents to atherosclerotic and thrombotic disease sites.[28,34,53-57] However, combination targeting of 'platelets + fibrin' to enhance clot-binding efficacy of nanoparticles has not been explored extensively. In fact, we found only one 'conference abstract' from almost 10 years ago that mention 'platelet and fibrin targeting' as a means to enhance ultrasound-responsive microbubble binding to thrombi for studying clot imaging and sonothrombolysis[58], but it does not state any comparative analysis of platelet-targeting vs fibrin-targeting vs combination targeting in the context of imaging or thrombolytic efficacy. In addition, this past study utilized antibodies and antibody fragments for targeting to platelets and fibrin, and such large molecules present significant steric challenge in decorating nanoparticle surfaces with sufficiently high number of 'ligand' copies. Therefore, we comparatively studied the effect of singular targeting (platelets or fibrin only) vs. combination targeting ('platelets + fibrin') using liposomes as model nanoparticles and small molecular weight peptides as ligands that can be incorporated on the surface at various densities.

Our computational studies and in vitro microfluidic studies clearly demonstrate that combination targeting of 'platelets + fibrin' provide substantially higher clot binding efficacy of nanoparticles compared to singularly targeting platelets or fibrin, even when the singularly targeted nanoparticles are mixed together. Our studies further indicate that for nanoparticles singularly targeted to platelets, the extent of nanoparticle binding to clots may keep increasing with higher ligand (e.g.

PBP) densities, suggesting that nanoparticles with increasing PBP mole % will either find more receptors on the platelet surface or find increasing number of platelets to bind within a clot with time. On the other hand, fibrin-targeted (FBP-decorated) nanoparticles reach a plateau of clot-anchorage at about 5 mole % ligand content, suggesting that these nanoparticles rapidly find the fibrin in the clots and reach a saturated level of binding. In contrast, nanoparticles bearing 'PBP + FBP' combinations find both platelets and fibrin to bind simultaneously and hence achieve a higher extent of clot-anchorage even at lower total ligand density. From a translation standpoint, higher ligand concentrations (hence densities) imply higher cost of materials and manufacturing of the clot-targeted nanoparticles, and hence combination targeting may provide a design approach for such nanoparticles that enables high extent of targeting but a lower cost (due to lower total ligand density). Also, our studies show that for such combination targeted nanoparticles the clot-anchorage capability actually goes down if the total ligand density is increased beyond a certain point (5 mole % in current studies). Our hypothesis is that this is due to a *'crowding'* effect of combination ligands above a certain optimal decoration density because of which they can potentially sterically inhibit nanoparticle binding to its target receptor motifs. In the framework of our *in vitro* studies we are utilizing a fixed volume of PRP with a consistent level of platelets and fibrinogen (thus fibrin) from which the clot is pre-formed in the microfluidic system. Therefore the amount of αIIbβ3 receptors (on platelets) and fibrin that the PBP and FBP ligands decorated on the nanoparticles can bind to, are somewhat constant. In this framework, the PBP-decorated particles can only bind to platelets, the FBP-decorated particles can only bind to fibrin, while the 'PBP + FBP'-decorated particles can bind to both platelets and fibrin. This 'combination targeting' thus leads to a higher extent of the PBP and FBP ligands 'finding' their substrate molecules to bind to. However, if the PBP and FBP decorations become too dense (*crowding* of ligands), then they can potentially sterically inhibit each other from binding to their respective target molecules, leading to an overall reduction of particle binding.

It is important to note that our studies reported here have certain limitations that in fact provide opportunities for further studies in the future. Firstly, in our computational studies we modeled a *pre-formed clot* where platelets have already aggregated by utilization of a certain percentage of αIIbβ3 crosslinked by fibrinogen and thus the binding of PBP to the available *free* αIIbβ3 is not being further inhibited by *free* fibrinogen in the model. We note that in the framework of an actively developing clot, the competition of *free* fibrinogen binding to available *free* αIIbβ3 will be a factor that will influence how many αIIbβ3 are available for PBP binding. Therefore, in our continued expansion of the computational studies, we are looking into modeling a 'developing clot' framework where PBP and fibrinogen can have equal probability of binding to αIIbβ3 and thus become incorporated in a 'competitive inhibition' framework based on PBP-nanoparticle vs fibrinogen concentration. These computational analyses are beyond the scope of the current report, and will be reported in future studies. Secondly, we have carried out all of our microfluidic studies under flow shear stress of 25 dyn/cm^2, since this shear condition can be considered as a middle zone between venous shear (low) and arterial shear (high).[59] Given the fact that the shear flow conditions can influence the binding kinetics of nanoparticles to targets especially in the vascular compartment, future studies can be directed to expand such systematic clot-targeting studies under venous vs. arterial flow conditions. Additionally, our flow volume consisted of nanoparticles suspended in saline and not plasma or whole blood. Past studies from our group as well as others have shown that while saline and plasma can be considered similar in flow dynamics, whole blood or presence of red blood cells would influence flow dynamics and particle distribution

significantly, where anisotropic non-spherical microparticles undergo higher margination to the wall and anchorage to target entities, compared to spherical nanoparticles.[60] These findings provide the opportunity to expand future studies of singular targeting vs. combination targeting in spherical vs. non-spherical particle platforms under plasma versus whole blood flow conditions. Also, our studies were performed with a fixed concentration (number) of nanoparticles across multiple comparison conditions. Future studies will also look at how increasing particle number without increasing ligand content/density per particle, can influence the overall clot-binding extent of the nanoparticles. While our studies show feasibility of achieving higher clot anchorage via combination targeting in vivo in a mouse arterial thrombus model, the expanded studies in the future can enable customized design of nanoparticle systems uniquely targeted to specific venous, arterial or microvascular disease sites for enhanced drug delivery in additional small and large animal models of acute and chronic thrombosis.

5. Conclusion

Using computational approaches as well as model microfluidic studies with liposomal nanoparticles and human blood clots, we demonstrate that combination targeting to 'platelets + fibrin' can provide enhanced efficacy of nanoparticle targeting to thrombi while utilizing lower extent of ligand density, compared to singularly targeting platelets only or fibrin only. Considering the fact that platelet and fibrin content, as well as their overall spatial distribution, can vary considerably between arterial vs. venous vs. microvascular thrombi, such combination targeting can provide a way to probabilistically ensure sufficient target availability and nanoparticle anchorage compared to singularly targeting systems. Such heteromultivalent design approach can be easily adapted to a variety of nanoparticle and microparticle systems to refine vascular drug delivery platforms. Beyond vascular drug delivery, the combination targeting strategy can become an attractive avenue of enhancing *active targeting* efficacy in any disease where the 'target profile' is often heterotypic, e.g. in thromboinflammation and in the tumor microenvironment.

Conflicts of Interest

There are no conflicts of interest to declare by any of the authors.

Acknowledgements

A. S. G and W. L. acknowledge funding by NIH R01 HL129179. T. S. and E. F. acknowledge funding by NSF CAREER 1564950 and NSF 1803693. W.L. also acknowledges support from R15-HL145573 and WV-INBRE grant. The work at Case Western made use of biomedical engineering research facilities built with funding from National Center for Research Resources Grant Number C06 RR12463-01 (PI: Kenneth Kutina). The cryo-TEM work made use of the EPIC facility of Northwestern University's NUANCE Center, which has received support from the Soft and Hybrid Nanotechnology Experimental (SHyNE) Resource (NSF ECCS-1542205) and the MRSEC program (NSF DMR-1720139). The content of this publication is solely the responsibility of the authors and does not represent the official views of the funding entities.

References

1. S. S. Virani, A. Alonso, E. J. Benjamin, M. S. Bittencourt, C. W. Callaway, A. P. Carson, A. M. Chamberlain, A. R. Chang, S. Cheng, F. N. Delling, L. Djousse, M. S. V. Elkind, J. F. Ferguson, M. Fornage, S. S. Khan, B. M. Kissela, K. L. Knutson, T. W. Kwan, D. T. Lackland, T. T. Lewis, J. H. Lichtman, C. T. Longenecker, M. S. Loop, P. L. Lutsey, S. S. Martin, K. Matsushita, A. E. Moran, M. E. Mussolino, A. M. Perak, W. D. Rosamond, G. A. Roth, U. K. A. Sampson, G. M. Satou, E. B. Schroeder, S. H. Shah, C. M. Shay, N. L. Spartano, A. Stokes, D. L. Tirschwell, L. B. VanWagner and C. W. Tsao for American Heart Association Council on Epidemiology and Prevention Statistics Committee and Stroke Statistics Subcommittee, Heart Disease and Stroke Statistics-2020 Update: A Report From the American Heart Association, *Circulation*, 2020, 141, e139-e596.

2. https://www.who.int/news-room/fact-sheets/detail/cardiovascular-diseases-(cvds)

3. G. Lippi, M. Franchini and G. Targher, Arterial thrombus formation in cardiovascular disease, *Nature Rev. Cardiol.*, 2011, 8, 502-512.

4. S. P. Jackson, Arterial thrombosis – insidious, unpredictable and deadly, *Nature Med.*, 2011, 17, 1423-1436.

5. A. S. Wolberg, F. R. Rosendaal, J. I. Weitz, I. H. Jaffer, G. Agnelli, T. Baglin and N. Mackman, Venous thrombosis, *Nature Rev. Disease Primers*, 2015, 1, 15006, doi: 10.1038/nrdp.2015.6.

6. M. V. Huisman, S. Barco, S. C. Cannegieter, G. Le Gal, S. V. Konstantinides, P. H. Reitsma, M. Rodger, A. Vonk Noordegraaf and F. A. Klok*, Pulmonary embolism, Nature Rev. Disease Primers, 2018, 4,* 18028, doi:10.1038/nrdp.2018.28.

7. D. D. Wagner and P. C. Burger, Platelets in inflammation and thrombosis, *Arterioscler. Thromb. Vasc. Biol.*, 2003, 23, 2131-2137.

8. M. Koupenova, B. E. Kehrel, H. A. Corkery and J. E. Freedman, Thrombosis and platelets: an update. *Eur. Heart J.*, 2017, 38, 785-791.

9. D. M. Monroe, M. Hoffman and H. R. Roberts, Platelets and thrombin generation, *Arterioscler. Thromb. Vasc. Biol.*, 2002, 22, 1381-1389.

10. S. Kattula, J. R. Byrnes and A. S. Wolberg, Fibrinogen and fibrin in hemostasis and thrombosis, *Arterioscler. Thromb. Vasc. Biol.*, 2017, 37, e13-e21.

11. R. A. S. Ariëns, T-S. Lai, J. W. Weisel, C. S. Greenberg and P. J. Grant, Role of factor XIII in fibrin clot formation and effects of genetic polymorphisms, *Blood*, 2002, 100, 743-754.
12. T. Urano, F. J. Castellino and Y. Suzuki, Regulation of plasminogen activation on cell surfaces and fibrin, *J. Thromb. Haemost*., 2018, 16, 1487-1497.

13. J. M. Connors and J. H. Levy, COVID-19 and its implications for thrombois and anticoagulation, *Blood*, 2020, doi: 10.1182/blood.2020006000. [Epub ahead of print].

14. J. F. Llitjos, M. Leclerc, C. Chochois, J. M. Monsallier, M. Ramakers, M. Auvray and K. Merouani, *J. Thromb. Haemost*., 2020, doi: 10.1111/jth.14869. [Epub ahead of print].

15. A. D. Michelson, Antiplatelet therapies as treatment for vascular disease, *Nature Rev. Drug Discovery*, 2010, 9, 154-169.

16. J. Park and Y. Byun, Recent advances in anticoagulant drug delivery, *Expert Opin. Drug. Del.*, 2016, 13, 421-434.

17. V. J. Marder, Historical perspective and future direction of thrombolysis research: the re-discovery of plasmin, *J. Thromb. Haemost.*, 2011, 9, 364-373.

18. N. Mackman, W. Bergmeier, G. A. Stouffer and J. I. Weitz, Therapeutic strategies for thrombosis: new targets and approaches, *Nature Rev. Drug Discovery*, 2020, 19, 333-352.

19. N. Tang, H. Bai, X. Chen, J. Gong, D. Li and Z. Sun, Anticoagulant treatment is associated with decreased mortality in severe coronavirus disease 2019 patients with coagulopathy, *J. Thromb. Haemost.*, 2020, 18, 1094-1099.

20. J. Wang, N. Hajizadeh, E. E. Moore, R. C. McIntyre, P. K. Moore, L. A. Veress, M. B. Yaffe, H. B. Moore and C. D. Barrett, Tissue Plasminogen Activator (tPA) treatment for COVID-19 associated acute respiratory distress syndrome (ARDS): A case series, *J. Thromb. Haemost.*, 2020, doi: 10.1111/jth.14828. [Epub ahead of print].

21. P. A. Gurbel and V. L. Serebruany, Oral Platelet IIb/IIIa inhibitors: From attractive theory to clinical failures, *J Thromb. Thrombolysis*, 2000,10, 217-220.

22. A. G. Rebeiz, C. B. Granger and M. L. Simoons. Incidence and management of complications of fibrinolytic, antiplatelet, and anticoagulant therapy, *Fundamental and Clinical Cardiology*, 2005, 52, 375-395.

23. M. A. Crowther and T. E. Warkentin, Bleeding risk and the management of bleeding complications in patients undergoing anticoagulant therapy, *Blood*, 2008, 111, 4871-4879.

24. E. L. Hellenbart, K. D. Falkenberg and S. W. Finks, Evaluation of bleeding in patients receiving direct oral anticoagulants, *Vasc. Health. Risk. Manage.*, 2017, 13, 325-342.

25. N. V. Deshpande, P. Admane and H. M. Mardikar, Bleeding on dual antiplatelet therapy: real life challenges, *Eur. Heart J. Suppl.*, 2018, 20, doi:10.1093/eurheartj/sux041.

26. J. W. Eikelboom and J. Hirsh, Bleeding and management of bleeding, *Eur. J. Heart J. Suppl.*, 2006, 8, G38-G45.

27. M. M. Levi, E. Erenberg, E. Löwenberg and P. W. Kamphuisen, Bleeding in patients using new anticoagulant or antiplatelet agents: risk factors and management, *Netherlands J. Med.*, 2010, 68, 68-76.

28. M. Sun and A. Sen Gupta, Vascular nanomedicine: Current status, opportunities and challenges, *Semin. Thromb. Hemost.*, 2019, doi: 10.1055/s-0039-1692395. [Epub ahead of print].

29. T. Huang, N. Li and J. Gao, Recent strategies on targeted delivery of thrombolytics, *Asian J. Pharm. Sci.*, 2019, 14, 233-247.

30. M. A. Berny, I. C. A. Munnix, J. M. Auger, S. E. M. Schols, J. M. E. M. Cosemans, P. Panizzi, P. E. Bock, S. P. Watson, O. J. T. McCarty, J. W. M. Heemskerk, Spatial distribution of Factor Xa, thrombin and fibrin(ogen) on thrombi at venous shear, *PLoS ONE*, 2010, 5, e10415.

31. M. Tomaiuolo, C. N. Matzko, I. Poventud-Fuentes, J. W. Weisel, L. F. Brass, T. J. Stalker, Interrelationships between structure and function during the hemostatic response to injury, *Proc. Nat. Acad. Sci.*, 2019, 116, 2243-2252.

32. A. R. Wufsus, N. E. Macera and K. B. Neeves, The hydraulic permeability of blood clots as a function of fibrin and platelet density, *Biophys. J.*, 2013, 104, 1812-1823.

33. I. N. Chernysh, C. Nagaswami, S. Kosolapova, A. D. Peshkova, A. Cuker, D. B. Cines, C. L. Cambor, R. I. Litvinov and J. W. Weisel, The distinctive structure and composition of arterial and venous thrombi and pulmonary emboli, *Sci. Rep.* 2020, 10, 5112.

34. A. Sen Gupta, G. Huang, B. J. Lestini, S. Sagnella, K. Kottke-Marchant and R. E. Marchant, RGD-modified liposomes targeted to activated platelets as a potential vascular drug delivery system, *Thromb. Haemost.*, 2005, 93, 106-114.

35. A. F. Kolodziej, S. A. Nair, P. Graham, T. J. McMurry, R. C. Ladner, C. Wescott, D. J. Sexton and P. Caravan, Fibrin specific peptides derived by phage display: Characterization of peptides and conjugates for imaging, *Bioconj. Chem.*, 2012, 23, 548-556.

36. I. Coin, M. Beyermann and M. Bienert, Solid-phase peptide synthesis: from standard procedures to the synthesis of difficult sequences. *Nature Protocols*, 2007, 2, 3247-3256.

37. S. Sachdeva, H. Joo, J. Tsai, B. Jasti and X. Li, A rational approach for creating peptides mimicking antibody binding. *Sci. Rep.,* 209, 9: 997.

38. D. C. Malaspina, G. Longo, I. Szleifer, Behavior of ligand binding assays with crowded surfaces: Molecular model of antigen capture by antibody-conjugated nanoparticles. *PLoS ONE*, 2017, 12: e0185518

39. A. L. Kuharsky and A. L. Fogelson, Surface-mediated control of blood coagulation: The role of binding site densities and platelet deposition, *Biophys. J.*, 2001, 80, 1050-1074.

40. S. L. Diamond and S. Anand, Inner clot diffusion and permeation during fibrinolysis, *Biophys. J.*, 1993, 65, 2622-2643.

41. O. Kononova, R. I. Litvinov, D. S. Blokhin, V. V. Klochkov, J. W. Weisel, J. S. Bennett and V. Barsegov, Mechanistic basis for the binding of RGD- and AGDV-peptides to the platelet integrin αIIbβ3, *Biochemistry*, 2017, 56, 1932-1942.

42. J. E. Woodell-May, D. N. Ridderman, M. J. Swift and J. Higgins, Producing accurate platelet counts for platelet rich plasma: Validation of a hematology analyzer and preparation techniques for counting, *J. Craniofacial. Surg.*, 2005, 16, 749-756.

43. J. S. Bennett, Structure and function of the platelet integrin αIIbβ3, *J. Clin. Invest.*, 2005, 115, 3363-3369.

44. G. D. O. Lowe, A. Rumley and I. J. Mackie, Plasma fibrinogen, *Ann. Clin. Biochem*., 2004, 41, 430-440.

45. H. Zhang, Thin-Film Hydration Followed by Extrusion Method for Liposome Preparation. In: D'Souza G. (eds) Liposomes. *Methods in Molecular Biology*, 2017, 1522, 17-22. Humana Press, New York, NY.

46. Z. Huang, M. R. Jaafari, F. C. Szoka Jr., Disterolphospholipids: Non-exchangeable lipids and their application to liposomal drug delivery, *Angew. Chem. Intl. Ed. Engl.*, 2009, 48, 4146-4149

47. S. P. Grover and N. Mackman, How useful are ferric chloride models of arterial thrombosis? *Platelets*, 2020, 31, 432-438.

48. W. Li, M. Nieman and A. Sen Gupta, Ferric Chloride-induced murine thrombosis models, *J. Vis. Exp.*, 2016, 115, 54479.

49. S. Hong, P. R. Leroueil, I. J. Majoros, B. G. Orr, J. R. Baker Jr. and M. M. B. Holl, The binding avidity of a nanoparticle-based multivalent targeted drug delivery platform, *Chemistry and Biology*, 2007, 14, 107-115.

50. R. X. Zhang, J. Li, T. Zhang, M. A. Amini, C. He, B. Lu, T. Ahmed, H. Y. Lip, A. M. Rauth and X. Y. Wu, Importance of integrating nanotechnology with pharmacology and physiology for innovative drug delivery and therapy – an illustration with first hand examples, *Acta Pharm. Sinica*, 2018, 39, 825-844.

51. C. Modery-Pawlowski and A. Sen Gupta, Heteromultivalent ligand-decoration for actively targeted nanomedicine, *Biomaterials*, 2014, 35, 2568-2579.

52. T. Curk, J. Dobnikar and D. Frenkel, Optimal multivalent targeting of membranes with many distinct receptors, *Proc. Nat. Acad. Sci.*, 2017, 114, 7210-7215.

53. J. N. Marsh, A. Senpan, G. Hu, M. J. Scott, P. J. Gaffney, S. A. Wickline and G. M. Lanza, Fibrin-targeted perfluorocarbon nanoparticles for targeted thrombolysis, *Nanomedicine*, 2007, 2, 533-543.

54. M.E. Klegerman, Y. Zou and D.D. McPherson, Fibrin targeting of echogenic liposomes with inactivated tissue plasminogen activator, *J Lipo. Res.*, 2008, 18, 95-112.

55. A. C. Brown, S. E. Stabenfeldt, B. Ahn, R. T. Hannan, K. S. Dhada, E. S. Herman, V. Stefanelli, N. Guzzetta, A. Alexeev, W. A. Lam, L. A. Lyon and T. H. Barker, Ultrasoft microgels displaying emergent platelet-like behaviours, *Nature Mater.*, 2014, 13, 1108-1114.

56. C. L. Pawlowski, W. Li, M. Sun, K. Ravichandran, D. Hickman, C. Kos, G. Kaur and A. Sen Gupta, Platelet microparticle-inspired clot-responsive nanomedicine for targeted fibrinolysis, *Biomaterials*, 2017, 128, 94-108.

57. C. Kang, S. Gwon, C. Song, P. M. Kang, S-C Park, J. Jeon, D. W. Huang and D. Lee, Fibrin-targeted and H_2O_2-respondive nanoparticles as a theranostics for thrombosed vessels. *ACS Nano*, 2017, 11, 6194-6203.

58. F. Xie, S. Gao, L. K. Drvol, E. Unger, S. Morehead, A. Kerschen, J. Lof and T. R. Porter, Effects of combined platelet and fibrin targeted microbubbles on the success of ultrasound an microbubble mediated thrombus dissolution of older thrombi, *Circulation*, 2010, 122, A10484.

59. T. G. Papaioannou and C. Steganadis, Vascular wall shear stress: Basic principles and methods, *Hellenic J. Cardiol.*, 2005, 46, 9-15.

60. M. Cooley, A. Sarode, M. Hoore, D. A. Fedosov, S. Mitragotri and A. Sen Gupta, Influence of particle size and shape on their margination and wall-adhesion: implications in drug delivery vehicle design across nano-to-micro scale, *Nanoscale*, 2018, 10, 15350-15364.

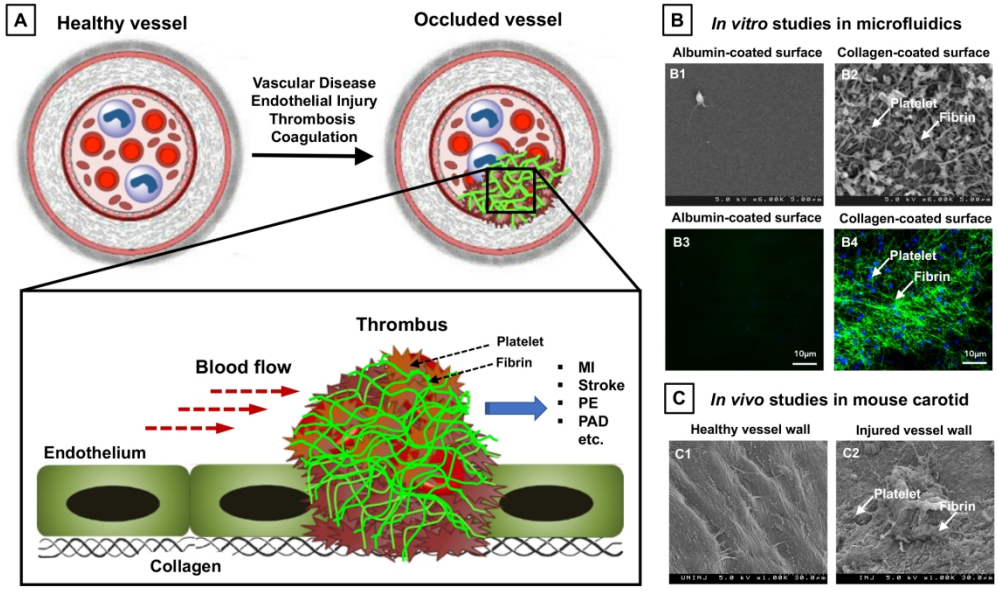

185x108mm (300 x 300 DPI)

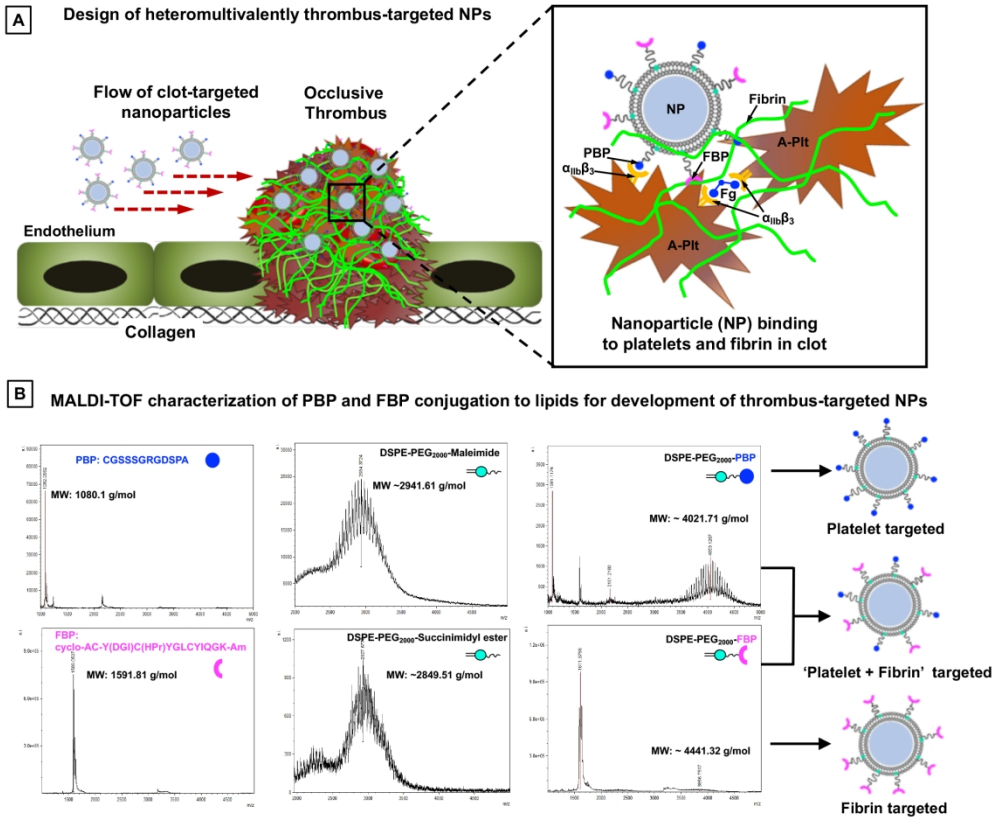

185x153mm (300 x 300 DPI)

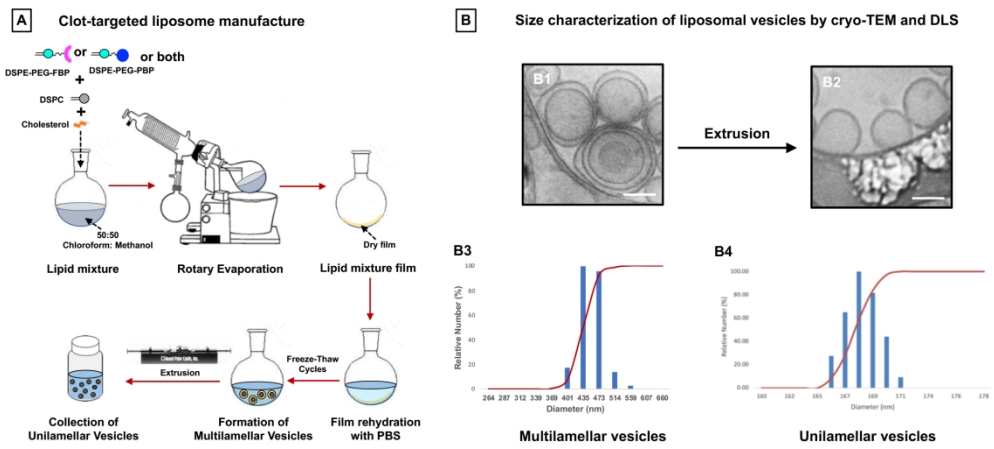

185x86mm (300 x 300 DPI)

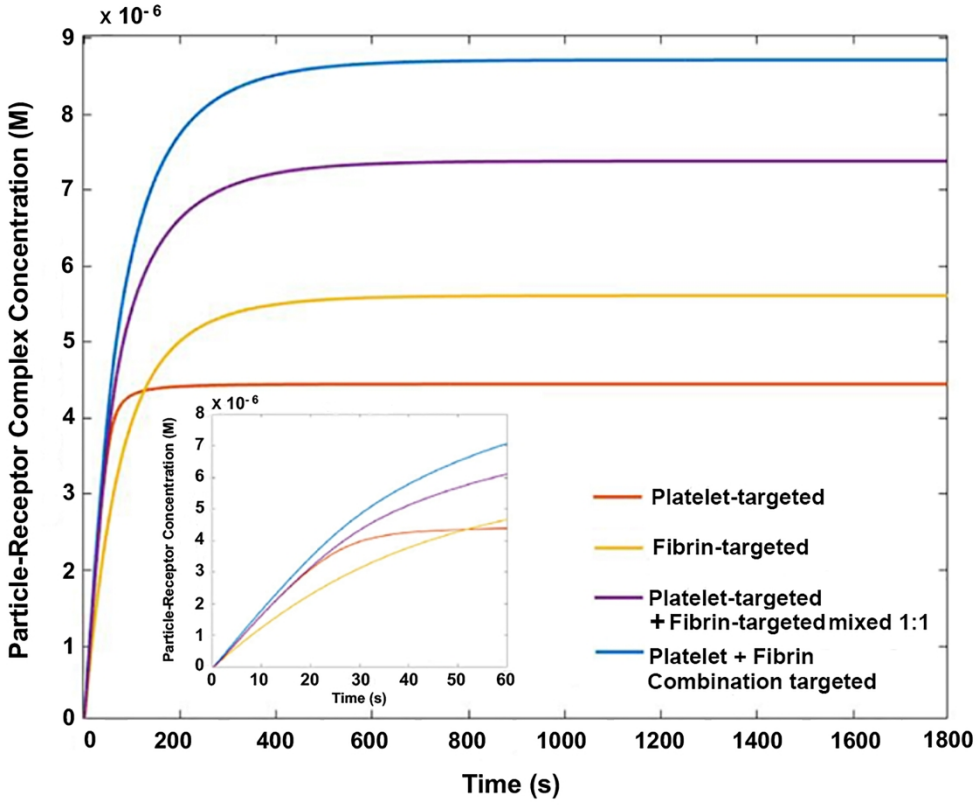

254x208mm (300 x 300 DPI)

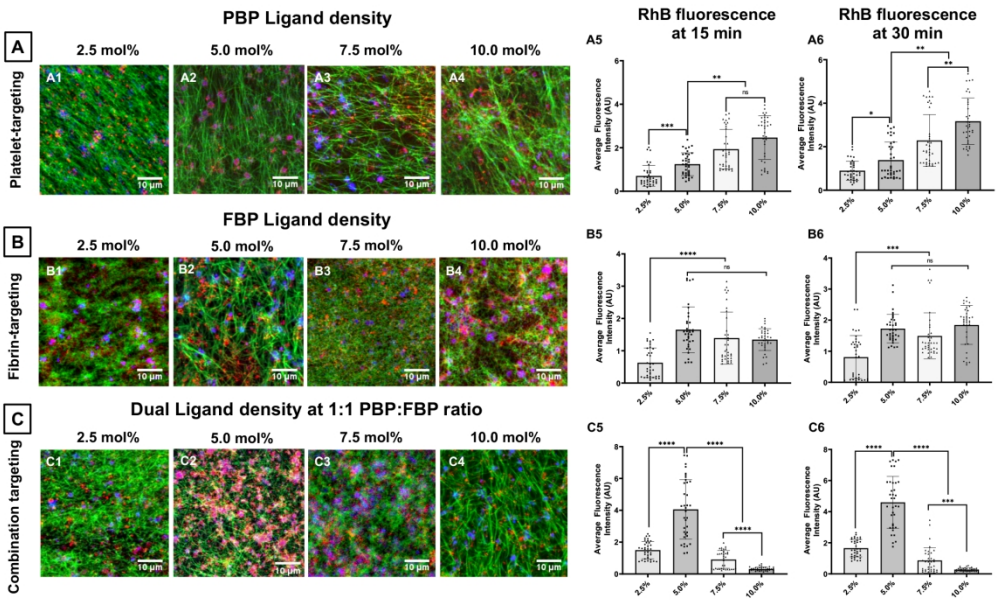

185x112mm (300 x 300 DPI)

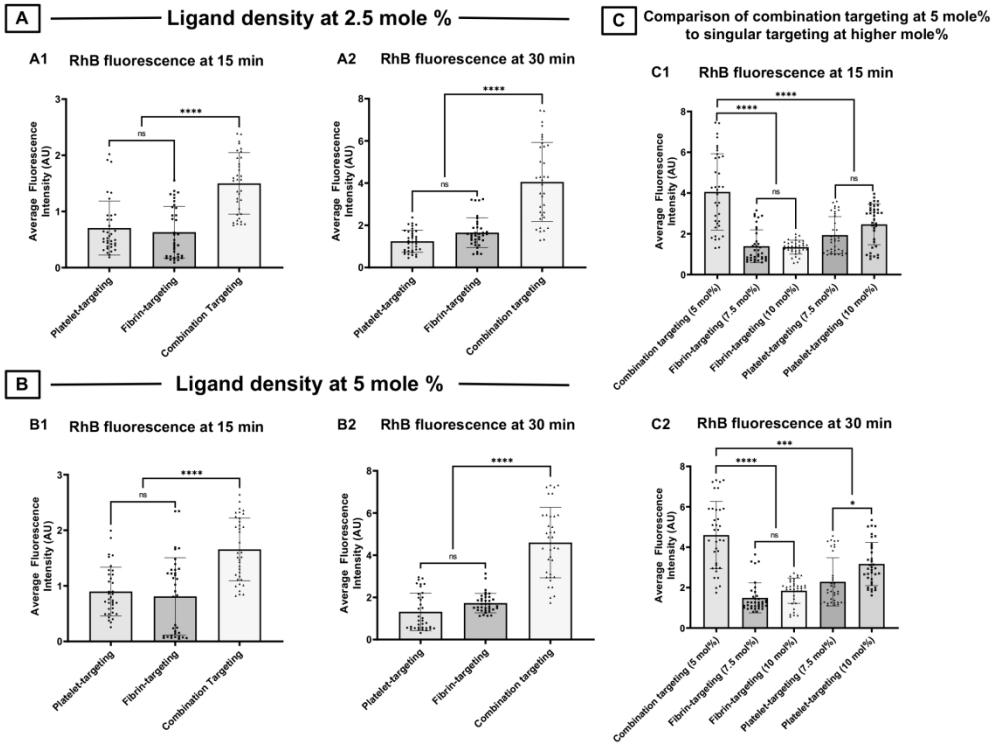

185x139mm (300 x 300 DPI)

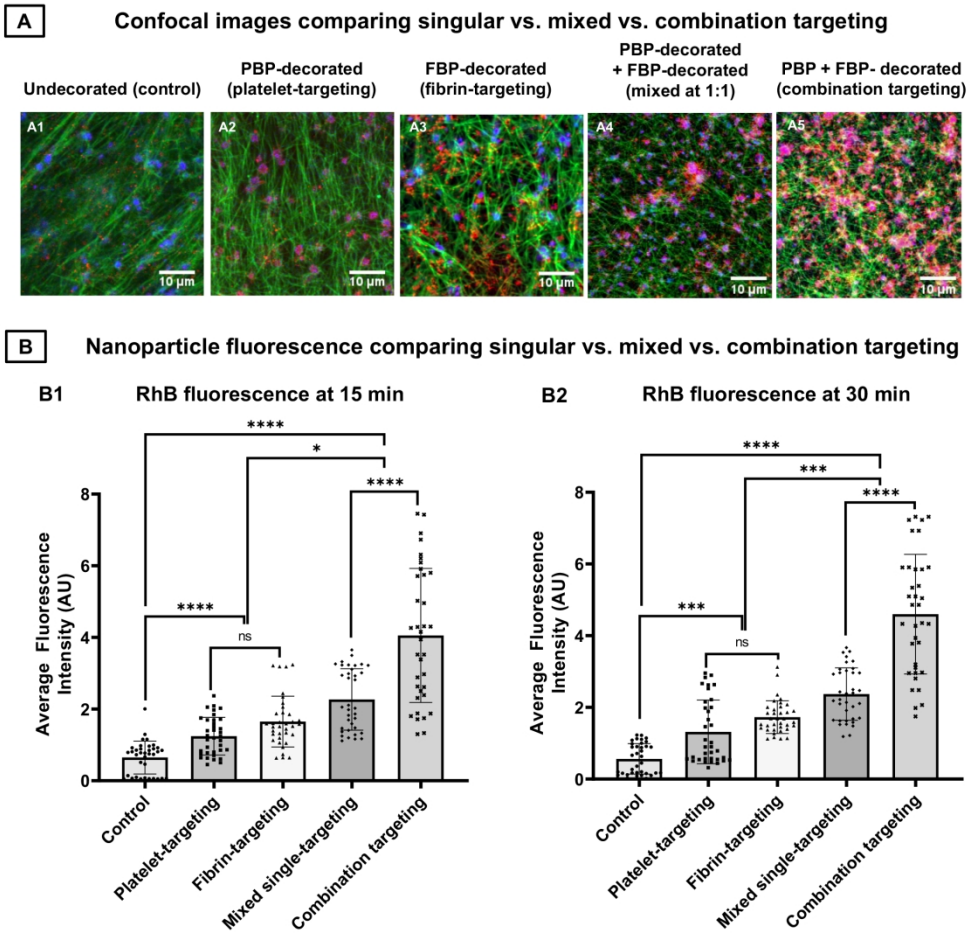

185x175mm (300 x 300 DPI)

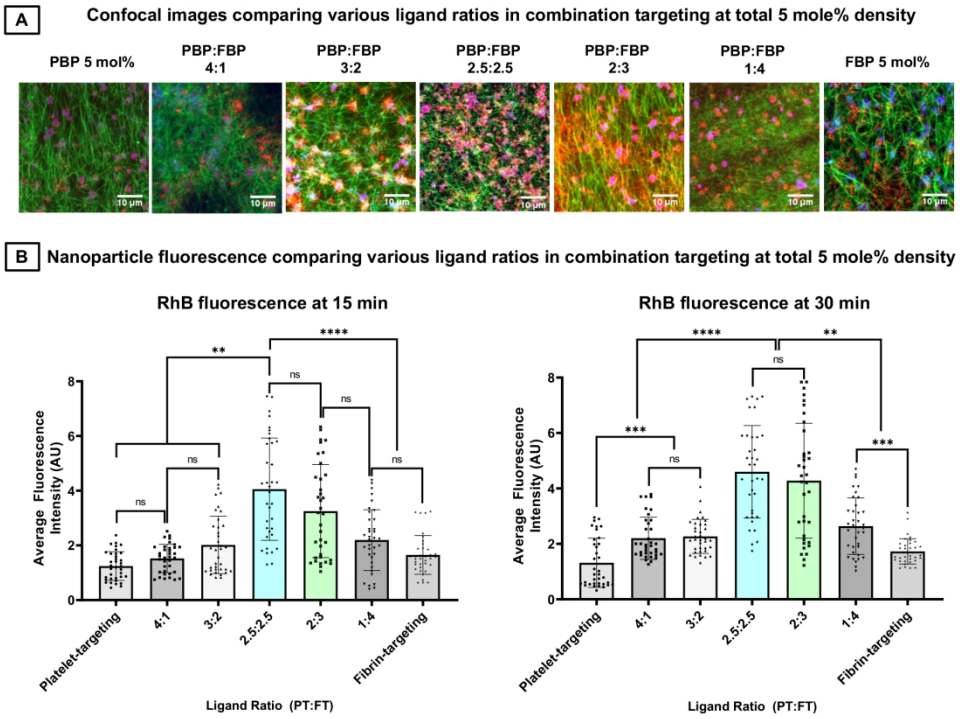

185x134mm (300 x 300 DPI)

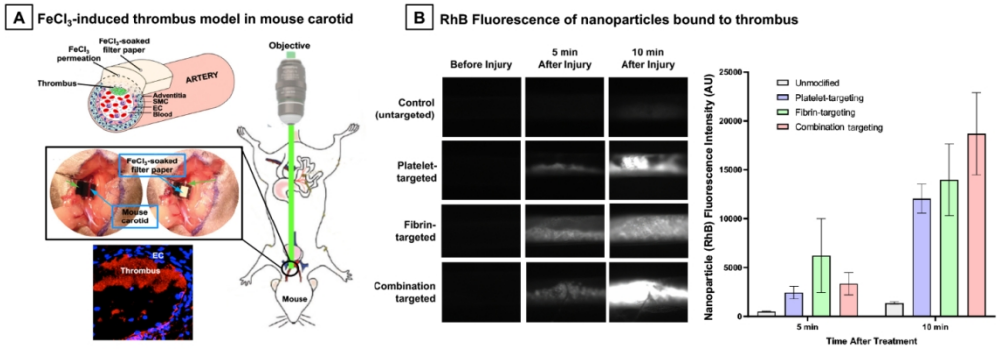

508x176mm (72 x 72 DPI)

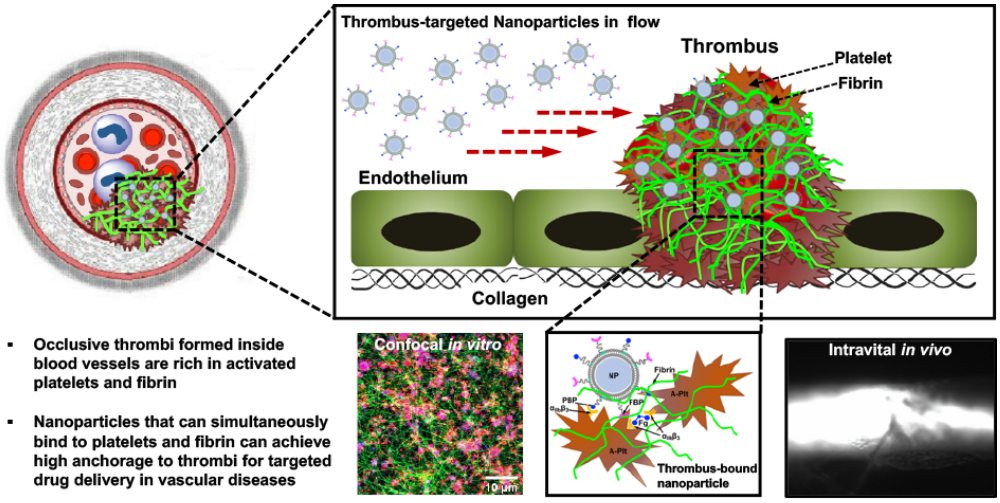

80x39mm (300 x 300 DPI)